

# Seismic Responses of Two RC Buildings and One Wood Building Based on an Input Wave Field

Masahiro Iida, A.M.ASCE<sup>1</sup>; Masanori Iiba<sup>2</sup>; Koichi Kusunoki<sup>3</sup>; Yuji Miyamoto<sup>4</sup>; and Hiroshi Isoda<sup>5</sup>

**Abstract:** A recently proposed three-dimensional (3D) linear method for examining soil-building interactions based on an input seismic wave field is, after some improvements, applied to estimate seismic building responses in the reclaimed zone of Tokyo Bay, where ground motions include a considerable amount of surface waves, thus reconfirming the effects of the method in a different situation. A seismic wave field involves seismic waves propagating in a 3D medium. The proposed method was developed with the goal of adequately treating seismic surface waves trapped by a (several-kilometers) deep underground structure in a soil-building interaction system. Two simulations were carried out. The first simulation successfully reproduced surface, downhole, and building accelerograms that were recorded at one borehole station during two medium-sized earthquakes. In the second simulation, seismic responses of a midrise RC model building and a wood model building were favorably calculated at the other borehole station for the 1923 Kanto earthquake. The building responses also were compared with those calculated by two standard response analyses, demonstrating the superiority of the proposed method. DOI: [10.1061/\(ASCE\)GM.1943-5622.0000444](https://doi.org/10.1061/(ASCE)GM.1943-5622.0000444). © 2014 American Society of Civil Engineers.

**Author keywords:** Structural dynamics; Three-dimensional analysis; Concrete structures; Wood structures; Soft soils; Soil-structure interactions; Surface waves; Underground structures.

## Introduction

A base-fixed building-response analysis has been performed in numerous studies. Certainly, this popular analysis has played a very important role in the analysis of building performance. However, it is possible for a building foundation to suffer heavy damage while the building superstructure sustains almost no damage. Even if consideration is restricted to the building's superstructure, this analysis has three weak points. First, soil-building interaction effects are not considered. Second, if the predominant period of the ground is longer than the fundamental period of the superstructure at a soft-soil site, the fundamental mode of the soil-building interaction system, which corresponds to the fundamental mode of the soil body of the system, is not properly taken into account. Third, although a surface-acceleration time history exerts the inertial force on the superstructure, ground motions do not act directly on the superstructure.

A soil-building interaction analysis is of great benefit to estimate the seismic response of a building with piles. An interaction analysis

overcomes the first and second weak points and is also able to improve the third weak point largely. Strong ground motions have been implicitly assumed to be S waves in the engineering community. However, a large amount of surface waves can be included in ground motions at a soft-soil site. Although the predominant periods of S waves and surface waves should be almost identical, the vertical amplitude distributions of these waves can be quite different in surface layers at a soft-soil site, as demonstrated in several studies (e.g., Iida and Kawase 2004; Iida et al. 2005). Therefore, it is necessary to identify both S waves and surface waves and to treat them separately.

In an interaction analysis, it is very difficult to treat short-period surface waves (less than a few seconds) reasonably because seismic surface waves are trapped by a (several-kilometers) deep underground structure. Exactly speaking, the vertical increase in the amplitude of short-period surface waves in a shallow underground structure (several tens of meters) depends strongly on the material properties of the deep structure in which the surface waves propagate. This means that surface-wave incidence into a shallow-soil model is not valid for surface waves trapped by a deep structure. This problem of surface waves was explained mathematically in a soil-response study by Iida (2006).

In this context, to treat short-period surface waves adequately in a building-response analysis, a three-dimensional (3D) linear FEM for examining soil-building interactions based on an input seismic wave field was proposed in a recent study by Iida (2013). An input seismic wave field means that the forces produced by body and surface waves propagating in the 3D soil volume of a soil-building interaction system are employed as external forces in the finite-element (FE) simulations. This new treatment of seismic external force was employed successfully for the first time in the previously mentioned soil-response study by Iida (2006). Using the proposed method, seismic responses of low- to high-rise RC model buildings were successfully calculated for a large earthquake at a soft-soil site in Mexico City, Mexico, where surface waves trapped by a deep structure are dominant. It also was revealed that a conventional

<sup>1</sup>Researcher, Earthquake Research Institute, Univ. of Tokyo, 1-1-1, Yayoi, Bunkyo-ku, Tokyo 113-0032, Japan (corresponding author). E-mail: iida@eri.u-tokyo.ac.jp

<sup>2</sup>Research Supervisor, Building Research Institute, 1, Tachihara, Tsukuba, Ibaraki 305-0802, Japan. E-mail: iiba-m@kenken.go.jp

<sup>3</sup>Associate Professor, Earthquake Research Institute, Univ. of Tokyo, 1-1-1, Yayoi, Bunkyo-ku, Tokyo 113-0032, Japan. E-mail: kusunoki@eri.u-tokyo.ac.jp

<sup>4</sup>Professor, Dept. of Architecture, Osaka Univ., 1-1 Yamadaoka, Suita, Osaka 565-0871, Japan. E-mail: miyamoto@arch.eng.osaka-u.ac.jp

<sup>5</sup>Professor, Research Institute for Sustainable Humanosphere, Kyoto Univ., Gokasho, Uji City, Kyoto 611-0011, Japan. E-mail: hisoda@rish.kyoto-u.ac.jp

Note. This manuscript was submitted on July 11, 2012; approved on September 2, 2014; published online on September 29, 2014. Discussion period open until March 1, 2015; separate discussions must be submitted for individual papers. This paper is part of the *International Journal of Geomechanics*, © ASCE, ISSN 1532-3641/04014093(10)/\$25.00.

**Table 1.** Summary of the Two Simulations

Simulation	Purpose	Earthquake	Station	Building
First	Recording reproduction	1983 Yamanashi ( $M_J = 6.0$ ) 1988 Tokyo ( $M_J = 6.0$ )	Toyo	2-Story RC real
Second	Building responses	1923 Kanto ( $M_J = 8.1$ )	Echujima	8-Story RC model 2-Story wood model

interaction analysis based on an input base motion was invalid for estimating building responses induced by surface waves.

In this study, the proposed method is, after some improvements, applied to estimate seismic building responses in the reclaimed zone of Tokyo Bay, where ground motion includes a considerable amount of surface waves, to reconfirm the effects of the method in a different situation. In a multilayered soil model subject to horizontal ground motions, the two simulations described in Table 1 were carried out. The two horizontal components of strong-motion recordings were used, and only the north-south components are displayed. The target-period range of engineering interest was mainly between 0.2 and 2.0 s.

The first simulation reproduced surface, downhole, and building accelerograms that were recorded at one (Toyo) borehole station during two medium-sized earthquakes on the basis of an input wave field estimated from the surface and downhole accelerograms. In the reproduction, soil damping and building damping also were evaluated. In the second simulation, seismic responses of a midrise RC model building and a wood model building were calculated at the other (Echujima) borehole station for the 1923 Kanto earthquake (earthquake magnitude  $M_J = 8.1$ ). Here,  $M_J$  means the magnitude determined by the Japanese Meteorological Agency. It is well known that the Kanto earthquake caused the heaviest damage to the Tokyo metropolitan area. The deep underground structural model used at the Echujima station, which was obtained in a previous study (Iida et al. 2005), is described in Table 2. It is characterized by a soft silty surface deposit with a thickness of about 30 m that covers the Kanto sedimentary basin. The building responses also were compared with those calculated by a base-fixed building-response analysis and by a conventional soil-building interaction analysis. The second simulation was designed to examine the influence of different input excitations on the seismic responses of the two buildings.

For clarity, the objectives of this study were as follows: first, a soil-response study (Iida 2006) demonstrated the effects of an input wave field on soil responses in the lakebed zone of Mexico City and in the reclaimed zone of Tokyo Bay. Next, a building-response study (Iida 2013) confirmed the effects of an input wave field on building responses in the lakebed zone. This study reinforces the building-response study in the reclaimed zone via improvements in the response method, application to a wood building, reproduction of real building recordings, and comparison with a base-fixed building-response analysis.

For reference, many soil-building interaction analyses have been performed in the reclaimed zone of Tokyo Bay and in the alluvial zone of the Tokyo metropolitan area. The soil properties of the two zones are similar. This is so because the reclaimed zone was produced by recovering land from shallow inner Tokyo Bay (approximately 25 m), whereas the alluvial zone was in a submarine environment in the past. Some of the interaction analyses (e.g., Ohta et al. 1978; Abe et al. 1984; Kobayashi 1989) were conducted effectively by employing the previously mentioned surface, downhole, and building accelerograms at the Toyo borehole station. However, none of the interaction analyses have taken surface waves into account.

**Table 2.** Deep Underground Structural Model Used at Echujima Station

Depth (m)	P-wave velocity (m/s)	S-wave velocity (m/s)	Density ( $t/m^3$ )	Damping coefficient
0–4	620	110	1.70	0.045
4–10	940	110	1.70	0.045
10–16	1,330	130	1.60	0.038
16–26	1,330	130	1.70	0.038
26–34	1,330	230	1.70	0.022
34–38	930	230	1.70	0.022
38–53	1,750	440	2.00	0.011
53–70	1,750	440	1.85	0.011
70–75	1,750	300	1.85	0.017
75–83	1,750	460	1.85	0.011
83–100	1,750	460	1.90	0.011
100–210	1,830	500	1.90	0.010
210–1,000	1,830	880	1.90	0.006
$\geq 1,000$	1,830	880	1.90	0.006

## Methods

In this section, a 3D linear time-domain FEM for examining soil-building interactions based on an input seismic wave field is explained. The new method, which was proposed and described in a recent study by Iida (2013), is improved in terms of surface-wave modeling and damping modeling in this study. The improvements are made based on building responses that were simulated in the study by Iida (2013). The following paragraphs describe only the fundamentals of and the improvements to the new method. A base-fixed building-response method for the building superstructure and a conventional method for examining soil-building interactions based on an input base motion, which are employed for comparison, are also described.

Fig. 1 illustrates the 3D superstructure-foundation-pile-soil systems used. Until now, numerous interaction systems have been proposed (e.g., Toki and Fu 1987; Reza Tabatabaiefar et al. 2013). The interaction systems used are basically the same as those employed in the study by Iida (2013), which were originally developed by Ishihara and Miura (1993) and Ishihara (1994). Their systems are similar to those used by Toki and Fu (1987). The lumped-mass stick building superstructure rests on a rigid-box foundation supported on piles. The superstructure is modeled as a shear-spring system, and sway and rocking of the foundation are considered. The horizontal degree of freedom of each story is coupled with the rocking degree of freedom at the foundation. Each pile is modeled by beam elements, and the soil volume is modeled by 3D rectangular prism elements. To allow the relative movement (slip) of the pile with respect to the soil, joint spring elements are attached to both edges of each beam element that forms the pile. The side and bottom boundaries of the soil volume are equipped with viscous dampers. The one-dimensional deep underground structures have no side boundaries.

The input excitations of the three methods are as follows: in the base-fixed response method, the surface accelerogram of a wave

field is used as an input surface motion. It exerts the inertial force on the superstructure. In the conventional method for examining soil-building interactions, the most basic technique is adopted: an input base accelerogram exerts the inertial force on the system. The input base accelerogram is calculated by elastic wave theory from an accelerogram obtained at the depth of a downhole sensor, assuming that all ground motions are S waves. In the new method employing an input wave field, vertically propagating plane S waves and horizontally propagating plane surface waves are imposed on the soil volume of the 3D ( $x, y, z$ ) system.

The first improvement of the new method is the estimation of a surface-wave field. As was explained mathematically in a soil-response study (Iida 2006), surface waves are characterized not only by the period-dependent vertical amplitude distribution but also by the period-dependent horizontal phase velocity (dispersion). After the improvement, only the period-dependent vertical amplitude distribution is taken into account.

The damping form of each method is as follows: in the base-fixed response method, constant modal-factor-type damping is used (damping coefficient  $h_{BF}$ ). In the conventional method for examining soil-building interactions, spatially constant Rayleigh-type damping of  $h_{MO} = h_1 = h_2$  is used, where  $h_1$  and  $h_2$  denote the damping coefficients evaluated at the primary and secondary predominant periods of the ground, respectively. In these two

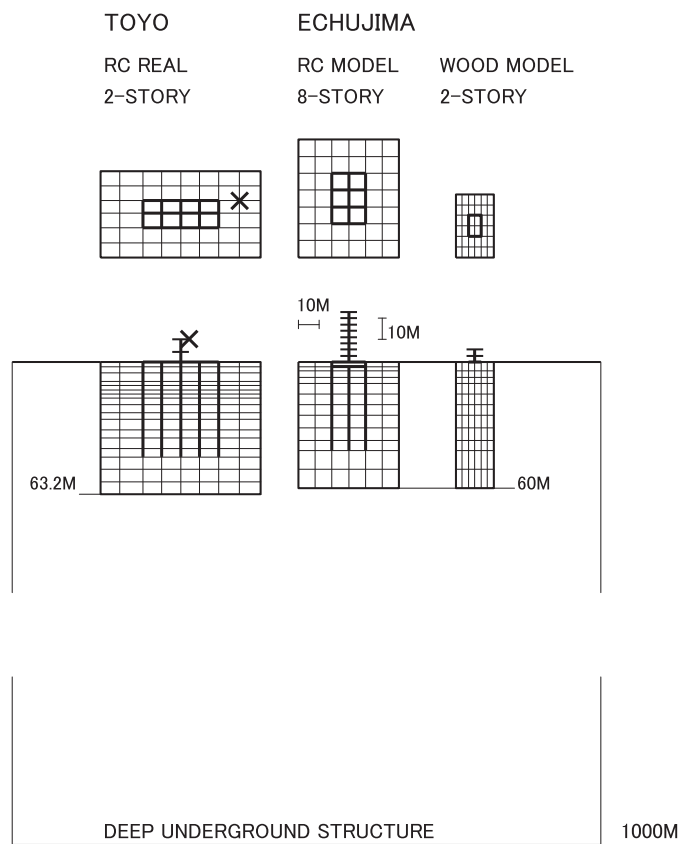


**Fig. 1.** Plan sections and cross sections (north-south direction) of the 3D superstructure-foundation-pile-soil systems for the three buildings (the right-hand side is the north direction, and horizontal and vertical scales of 10 m are given; regarding the RC building, the cross mark on the plan section shows a vertical array, and the cross mark on the cross section indicates a building sensor; one-dimensional appropriate deep underground structures without side boundaries, which are used to estimate input wave fields, are also displayed)

methods, typical damping coefficients are assumed on the basis of experience.

The second improvement of the new method is the damping form. Because the new method has not been applied extensively, the following spatially variable Rayleigh-type damping matrix is employed:

$$[C] = 2\omega_1 [H_M][M] + 2/\omega_1 [H_K][K]$$

where  $[M]$  = mass matrix;  $[K]$  = stiffness matrix;  $[H_M]$  and  $[H_K]$  = matrices of the damping coefficients associated with the mass and stiffness, respectively; and  $\omega_1$  = primary angular frequency of the ground. Here,  $h_{WFij} = h_{Mij} = h_{Kij}$  is assumed, where  $h_{Mij}$  and  $h_{Kij}$  are the elements that lie in the  $i$ th row and the  $j$ th column of matrices  $[H_M]$  and  $[H_K]$ , respectively. The spatially variable damping coefficients  $h_{WF}$  are determined experimentally.

### Reproduction of Building Recordings

In this section, the new method is applied to reproduce the surface, downhole, and building accelerograms recorded during the 1983 Yamanashi ( $M_J = 6.0$ ) and the 1988 Tokyo ( $M_J = 6.0$ ) earthquakes at the Toyo borehole station, where building observation was performed along with ground observation (Fig. 2). The Toyo station is the only station available for reproducing building recordings in the reclaimed zone of Tokyo Bay.

In a previous study by Iida et al. (2005), the nature of ground motions was investigated by a systematic analysis of accelerograms recorded during several medium-sized earthquakes at two coastal borehole stations (Toyo and Echujima) where the two simulations of this study were carried out. The previous study clarified that Love waves were more dominant at the Echujima station than at the Toyo station, so the amplitudes of surface recordings at the Echujima station were considerably larger than those at the Toyo station. For

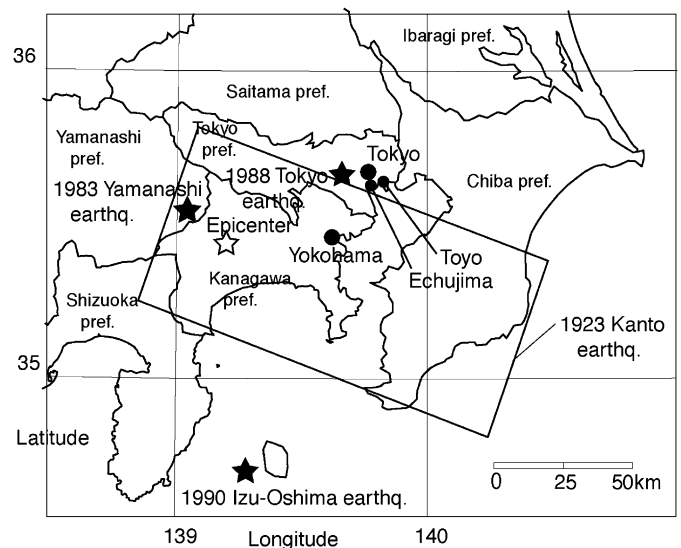


**Fig. 2.** Location map of the Kanto region of Japan (the surface-fault geometry of the 1923 Kanto earthquake is projected, and the epicenter is indicated by an open star; the epicenters of three medium-sized earthquakes are marked with solid stars; the Toyo and Echujima borehole stations are shown by small solid circles) (adapted from Iida 2006, © ASCE)

this reason, building responses during the 1923 Kanto earthquake were calculated at the Echujima station, as noted in the next section.

For example, the top trace in Fig. 3 exhibits the surface accelerogram recorded at the Toyo borehole station during the 1983 Yamanashi earthquake. The surface accelerogram is a typical recording observed at a soft-soil site, and ground motions are dominant at periods of around 1.0 s. Judging from the small amplitudes of the accelerograms recorded at the Toyo station, the soil and building responses calculated in this section should remain in the linear range.

### Building Model

Fig. 1 shows the interaction system for an instrumented 2-story RC real building at the Toyo borehole station. In the horizontal extent of the system, it was confirmed that artificial wave reflections caused by the side boundaries were negligible, which was described in detail in the recent study by Iida (2013). Parameters used for the superstructure and the foundation of the real building are summarized in Table 3 (Architectural Institute of Japan 1985). The two fundamental periods of two orthogonal orientations are evaluated under a base-fixed condition. Unusually, the 2-story RC building has long piles. The building vibrates with the secondary theoretical predominant period of the ground of 0.8 s (Fig. 4). Because of computational difficulty, the thin (1.4-m) embedment of the foundation was not considered, and a foundation model without the embedment was adopted.

Parameters used for the piles of the real building are summarized in Table 4 (Architectural Institute of Japan 1985). Throughout this study, the horizontal stiffness of the joint spring element that connects a node for the pile and another node for the soil was set to be  $10^9$  kN/m, and the vertical stiffness was set to be  $10^6$  and  $10^5$  kN/m at the tip and other beam elements, respectively. These values are

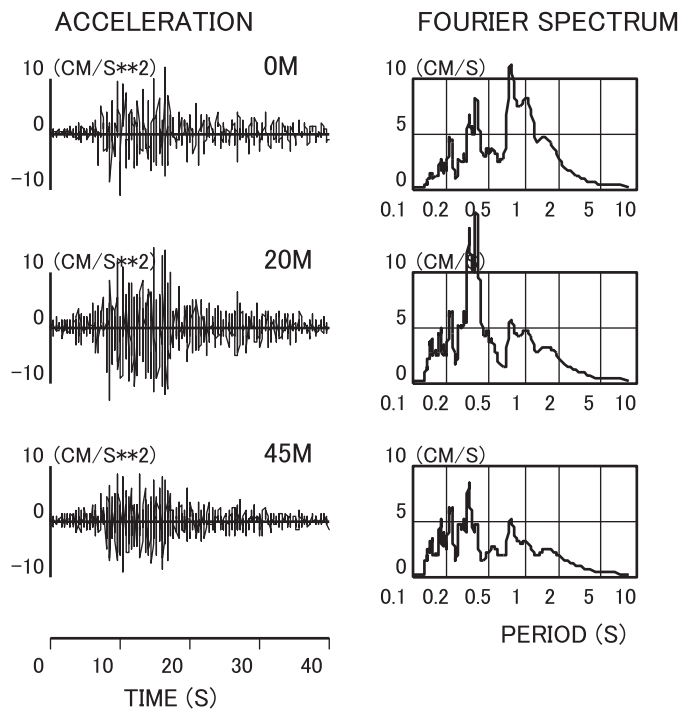


**Fig. 3.** Theoretical accelerograms at three depths (wave field) estimated at the Toyo station for the 1983 Yamanashi earthquake (surface accelerogram is the observed recording)

**Table 3.** Parameters Used for Superstructures and Foundations of the Three Buildings

Building	Superstructure				Foundation			
	Height of each story (m)	Mass of each story (t)	Stiffness of each story (kN/m)	Yield shear strength of each story (kN)	Fundamental period (s)	Mass (t)	Embedment (m)	Length, width (m)
2-Story RC real	5.8 (2)	611 (2)	$8.22 \times 10^6$ (2,NS)	—	0.09 (NS)	518	0	36, 13
	4.6 (1)	741 (1)	$2.84 \times 10^6$ (2,EW)		0.12 (EW)			
8-Story RC model	3	509	$8.72 \times 10^6$ (1,NS)	4,988 (4-8)	0.68	408	2	24, 16
			$7.11 \times 10^6$ (1,EW)	6,987 (3)				
2-Story wood model	2.7	5.6 (2)	$1.20 \times 10^6$ (4-8)	9,290 (2)	0.74	37	0	10, 6
		10.2 (1)	$1.23 \times 10^6$ (3)	11,976 (1)				
			$1.27 \times 10^6$ (2)	16.1 (2)				
			$1.66 \times 10^6$ (1)	37.8 (1)				

Note: Numerical values in parentheses are story numbers.

exactly the same as those employed in the study by Iida (2013) and worked well in this study.

### Wave Field

First, using the soil volume of the 3D interaction system for the real building, an input wave field was estimated from the separated surface S- and surface-wave accelerograms and the deep structural model (Fig. 1), which were obtained in the previously mentioned ground-motion study (Iida et al. 2005). Fig. 3 displays the wave field estimated at the Toyo station for the 1983 Yamanashi earthquake. The depth of 20 m corresponds to the soft-soil sediment, and the depth of 45 m corresponds to the sediment-bedrock interface. A large vertical increase in the amplitudes is seen in the soft surface layers at periods greater than 0.8 s.

### Soil Responses

Second, to confirm good reproduction of an input wave field by soil responses, a preparatory soil response analysis was conducted. Reflecting ground motions at the soft-soil site, the recorded building accelerograms did not contain a lot of short-period components, so a soil-response analysis was performed at periods greater than 0.2 s. In this study, the soil- and building-response analyses were performed for 40 s with a time interval of 0.01 s. Fig. 5 displays the FE-simulated soil responses based on the input wave field estimated for the 1983 Yamanashi earthquake. After some trial and error, given a damping coefficient  $h_{WF}$  of 0.16 for the soil layers above 28 m deep and another damping coefficient  $h_{WF}$  of 0.10 for the soil layers below 28 m deep, the input wave field of Fig. 3 was retrieved fairly well. The large damping coefficients are derived from the external force of an input wave field.

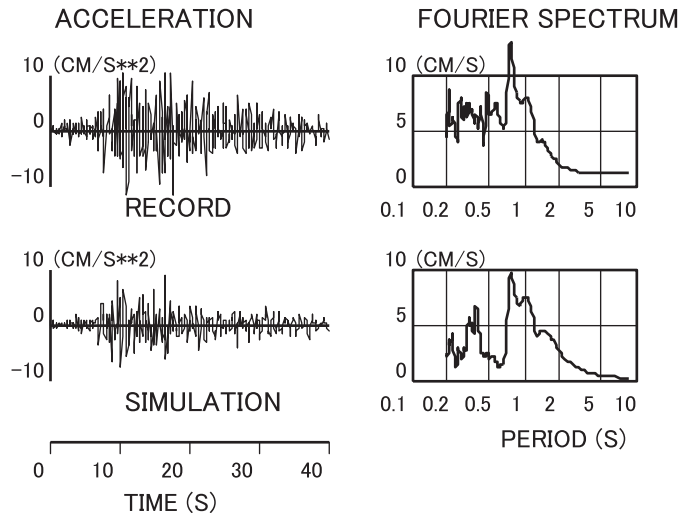


**Fig. 4.** Recorded and simulated top-story accelerograms of the 2-story RC real building at the Toyo station for the 1983 Yamanashi earthquake (simulated absolute accelerogram includes rocking)

### Building Responses

Finally, a 3D soil-building interaction analysis based on an input wave field was performed. Fig. 4 compares the recorded and simulated top-story accelerograms for the 1983 Yamanashi event, which are displayed in an effective-period range greater than 0.2 s for rigorous comparison. In this simulation, a damping coefficient  $h_{WF}$  of 0.05 was assigned for the real building.

The spectral peak at a period of 0.8 s in the simulated accelerogram coincided well with that in the recorded accelerogram. Moreover, the spectrum of the simulation matched well with that of the recording in the long-period range of more than 0.8 s. This means that the simulation works well around the primary and secondary theoretical predominant periods (1.5 and 0.8 s) of the ground. The fundamental period (0.1 s) of the building (Table 3) is much shorter. On the other hand, the amplitudes of the simulated accelerogram were considerably smaller than those of the recorded accelerogram because of the lack of high-frequency motions. There are several possible reasons for this inconsistency: (1) the building model might not be realistic enough, (2) the wave field might not be very accurate, or (3) the one-dimensional soil modeling might not be sufficient. However, the real reasons are uncertain.

Thus, although high-frequency motions cannot be reproduced well by the simulation, the new method basically works well. The reproduction of building recordings should be further required, using surface, downhole, and building recordings obtained in another area. The damping coefficient assigned for the real building will be used for two model buildings in the next section.

### Comparison with Two Other Methods

In this section, the seismic responses of a midrise RC model building and a wood model building are calculated at the Echujima borehole station for the 1923 Kanto earthquake. The building responses calculated by the new method are compared with those calculated by the previously mentioned two standard methods. In a soil-response study (Iida 2006), surface S- and surface-wave accelerograms were synthesized with an empirical Green's function summation technique at the Echujima station for the Kanto earthquake. The surface fault geometry of the event is shown in Fig. 2, and the fault zone covers much of the Tokyo metropolitan area. The accelerograms recorded during three medium-sized events, which are marked with black stars in Fig. 2, were used as Green's functions.

The synthesized S-wave accelerograms had larger amplitudes than the synthesized surface-wave accelerograms. On the other hand, around the theoretical predominant period of the ground of 1.2 s, surface waves were dominant rather than S waves. As summations of the S- and surface-wave accelerograms, the synthesized surface whole-wave accelerograms had a large spectral peak at the predominant period. The synthesized accelerogram is displayed as the top trace of Fig. 6. The very large amplitudes of the accelerogram are probably the result of linear soil modeling. It is anticipated that a midrise RC building and a wood building will shake severely at the station because the two buildings resonate with the predominant

**Table 4.** Parameters Used for Concrete-Filled Steel Piles of the Two RC Buildings

Building	Number	Length (m)	Radius (m)	Elastic modulus (kN/m <sup>2</sup> )	Density (t/m <sup>3</sup> )	Pure yield bending moment <sup>a</sup> (kN · m)	Maximum yield bending moment (kN · m)
2-Story RC real	15	45.4	0.50 (outer piles) 0.55 (inner piles)	$2.94 \times 10^7$	2.4	—	—
8-Story RC model	12	40	0.5	$1.47 \times 10^7$	2.4	1,600	2,600

<sup>a</sup>Pure yield bending moment means yield bending moment without axial force.

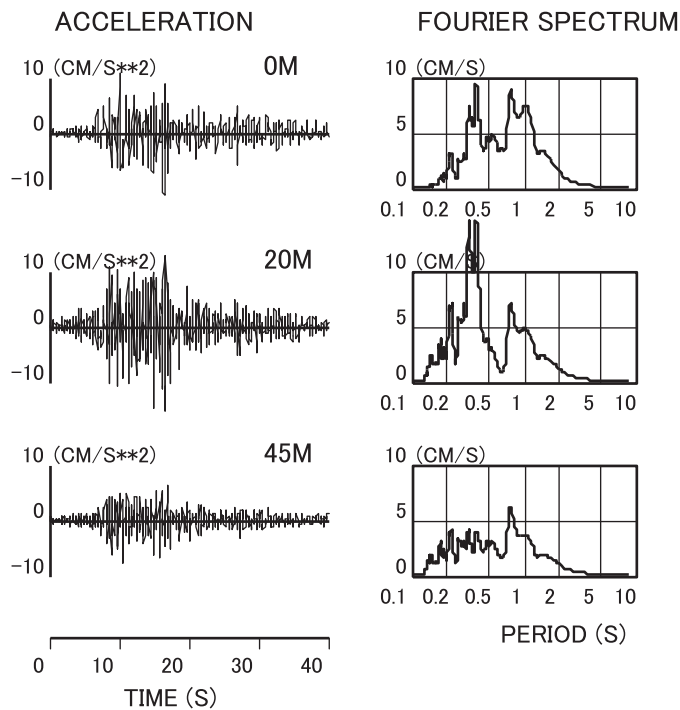


**Fig. 5.** FE-simulated soil responses at three depths based on the input wave field estimated at the Toyo station for the 1983 Yamanashi earthquake

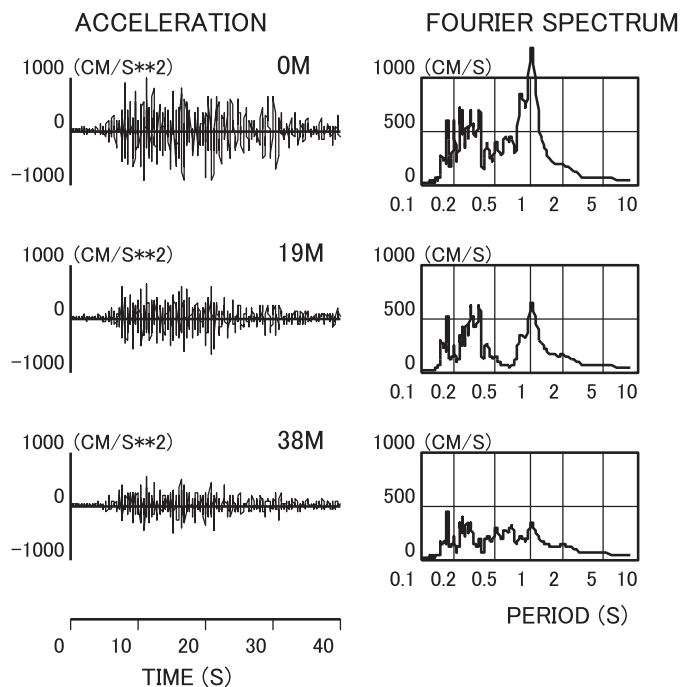


**Fig. 6.** Theoretical accelerograms at three depths (wave field) estimated at the Echujima station for the 1923 Kanto earthquake

period. The building responses will be beyond the linear range during the event.

In the soil-response study, an input base motion and an input wave field for a 3D soil model were estimated at the Echujima station for the Kanto earthquake. Moreover, linear soil responses were calculated using the input base motion and input wave field. It was

confirmed that the soil responses obtained using the input wave field reproduced the wave field much better than those using the input base motion.

### Building Model

Typical model buildings based on Japanese building codes were employed (Building Center of Japan 2013). Fig. 1 shows the 3D interaction systems for an 8-story RC model building and a 2-story wood model building. To decrease the computational burden, the model buildings have small foundation dimensions. Further, in the horizontal extent of the systems, it was confirmed that artificial wave reflections caused by the side boundaries were negligible. Parameters used for the superstructures and foundations of the two model buildings are summarized in Table 3. Parameters used for the piles of the 8-story RC model building are listed in Table 4.

Regarding the 8-story RC model building, a base shear coefficient  $D_s$  of 0.30 was supposed. Triangular distributions were assumed for the stiffness and shear strength, and for the stiffness, the yield stiffness was used. The parameter values of the top five stories were set to be equal to those of the fourth story. Because the pile tip needs to reach stiff-soil layers, a pile length of 40 m is required. The pile radius was determined such that the piles support the total mass of the superstructure and foundation.

On the other hand, the layout of the plan section of a wood building is arbitrary, so the structural parameters have large variations. Also, the foundation of a wood building is designed independently of the light superstructure. Hence, the 2-story wood building used here should be considered to be one typical example. The foundation without piles was fixed to the soil. Because of computational difficulty, the thin (0.5-m) embedment of the foundation was not considered, and a foundation model without the embedment was adopted.

### Wave Field

First, using the soil volume of the 3D interaction system for the 8-story RC model building, an input wave field for the Kanto earthquake was estimated from the synthesized surface S- and surface-wave accelerograms and the deep structural model of Table 2 (Fig. 1), which were obtained in the previously mentioned soil-response study by Iida (2006) and in a previous ground-motion study by Iida et al. (2005). Fig. 6 shows the wave field estimated at the Echujima station. The depth of 19 m corresponds to the soft-soil sediment, and the depth of 38 m corresponds to the sediment-bedrock interface. The vertical increase in the amplitudes gets very large near the ground surface at the predominant period of the ground.

### Soil Responses

Second, a preparatory soil-response analysis was conducted. The effective-period range of this soil-response analysis is greater than 0.2 s. In the conventional interaction analysis, the accelerogram evaluated on the bottom boundary (60 m deep) of the interaction system is used as an input base motion. To obtain the accelerogram, all ground motions were assumed to be S waves, and an accelerogram was synthesized with an empirical Green's function summation technique at the depth of a downhole sensor (40 m) at the Echujima station for the Kanto earthquake. The synthesized accelerogram was used as an input base motion because the structure between 40 and 60 m deep remains basically unchanged (Table 2). Also, a spatially constant damping coefficient of  $h_{MO} = 0.02$  was assumed for the entire system. Although this damping coefficient should be underestimated for the soft-soil sediment (Iida et al. 2005),

extremely small damping was required to gain apparently appropriate soil responses.

The FE-simulated soil responses based on the input base motion (Fig. 7) were extreme underestimations around the predominant period of the ground despite the assumed small soil damping. Fig. 8 displays the FE-simulated soil responses based on the input wave

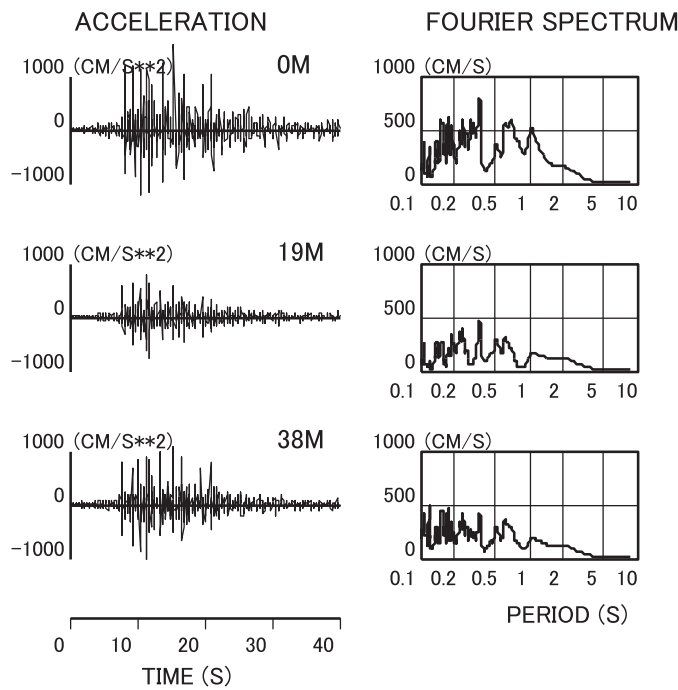


**Fig. 7.** FE-simulated soil responses at three depths based on the input base motion estimated at the Echujima station for the 1923 Kanto earthquake

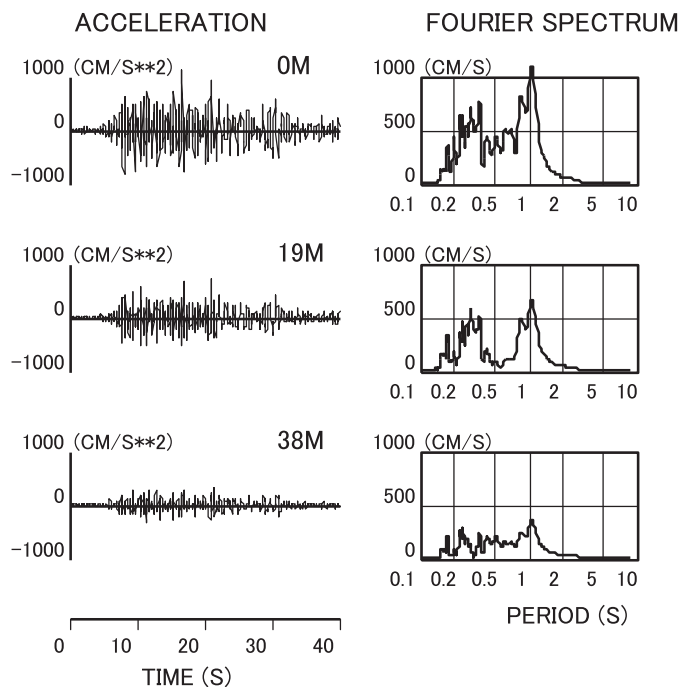


**Fig. 8.** FE-simulated soil responses at three depths based on the input wave field estimated at the Echujima station for the 1923 Kanto earthquake

field. Given a damping coefficient  $h_{WF}$  of 0.16 for the soil layers above 38 m deep and another damping coefficient  $h_{WF}$  of 0.10 for the soil layers below 38 m deep, the input wave field of Fig. 6 was retrieved very well.

### Building Responses

Finally, the building responses were computed by the three types of analyses. In the base-fixed response analysis, the surface accelerogram of the input wave field was used as the input surface motion. The surface accelerogram is displayed as the top trace of Fig. 6. A damping coefficient of  $h_{BF} = 0.05$  was assumed for the superstructure. In the new interaction analysis, a damping coefficient  $h_{WF}$  of 0.05 was assigned for the two model buildings. Thus, because linear building responses are being computed, the same damping coefficients were adopted between the RC and wood model buildings in each response analysis.

Table 5 summarizes the maximum response values of the superstructures of the two model buildings calculated by the three types of analyses. In all analyses, the top-story accelerations and displacements of the two model buildings became very large. Both model buildings suffered large interstory drifts that implied structural collapse and did not have enough shear strength to resist the severe vibration in the first story. In particular, the interstory drifts of the wood model building grew excessively large. In the base-fixed response analysis, the responses of the 2-story wood building became relatively small, presumably because the use of input surface motion as the inertial force is unreasonable for the light flexible superstructure. In the conventional interaction analysis, because of the biased ground motions, the responses of the 8-story RC model building were considerably underpredicted.

For more clarity on the influence of different input excitations, Figs. 9 and 10 compare the Fourier amplitude ratios between the top-story and foundation accelerograms of the 8-story RC model building and the 2-story wood model building, respectively. The interaction effects of the RC model building were recognized by the extended vibration period, whereas those of the wood model building were ambiguous. In the new interaction analysis, the spectral peaks were very sharp. The sharp peaks may show that realistic vibration of the buildings was properly expressed. Another possibility is that the building damping may be underestimated.

Next, Figs. 11 and 12 display the vertical distributions of the maximum interstory drift and the maximum shear force of the RC model building and the wood model building, respectively. In all the analyses, the shear force of each story of both buildings exceeded the yield strength by far, and the lower stories sustained extremely large shear force. It should be noted that the distribution patterns of the 8-story RC model building were highly different among the three types of analyses. The difference in the distribution patterns of the 2-story wood model building was not obvious.

Furthermore, Table 6 summarizes the maximum response values at the head of a corner pile of the 8-story RC model building calculated by the two types of interaction analyses. Fig. 13 compares the vertical distributions of the maximum bending moment of the same corner pile calculated by both analyses. It was found that the largest bending moment at the head was beyond the two sorts of yield bending moments of Table 4 in both analyses and that the largest bending moment calculated by the new analysis was larger than that calculated by the conventional analysis.

In addition, the pile response was calculated by the new analysis on the condition that only the superstructure was removed from the interaction system. The maximum response values at the head of the same corner pile are also shown in Table 6. The additional calculation clarified that about one-fourth of the shear force and the

**Table 5.** Maximum Response Values of Superstructures of the Two Model Buildings Calculated by the Three Types of Analyses at the Echujima Station for the 1923 Kanto Earthquake

Building	Analysis	Top-story acceleration (cm/s <sup>2</sup> )	Top-story displacement (cm)	Maximum interstory drift through all stories (cm)	Ratio of shear force to yield strength of first story (%)
8-Story RC model	Fixed	2,811	19.3	3.7	515
	Conventional	2,160	19.4	3.9	469
	New	2,905	40.2	7.2	795
2-Story wood model	Fixed	1,824	26.8	14.5	580
	Conventional	3,056	32.4	23.4	881
	New	3,191	48.2	25	1,031

Note: Neither the top-story absolute accelerations nor the top-story relative displacements with respect to the foundation include rocking.

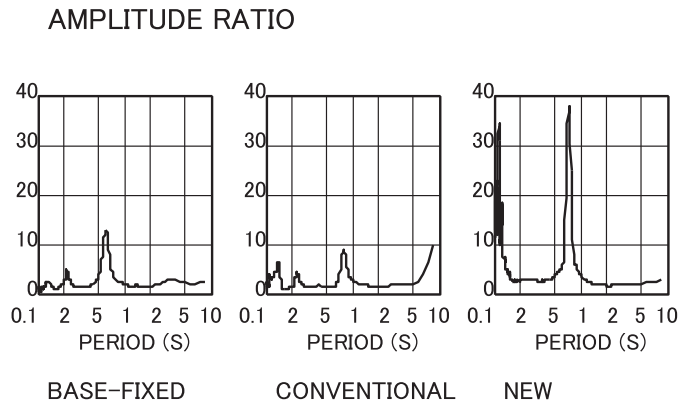


**Fig. 9.** Fourier amplitude ratios between top-story and foundation accelerograms of the 8-story RC model building calculated by the three types of analyses at the Echujima station for the 1923 Kanto earthquake (absolute accelerograms include no rocking)

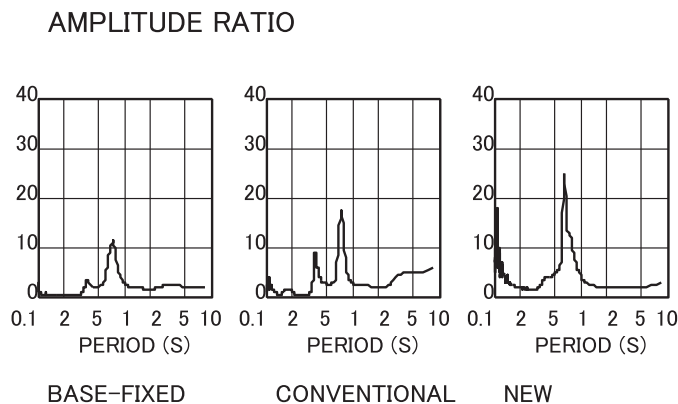


**Fig. 10.** Fourier amplitude ratios between top-story and foundation accelerograms of the 2-story wood model building calculated by the three types of analyses at the Echujima station for the 1923 Kanto earthquake (absolute accelerograms include no rocking)

bending moment was attributed to ground motions. The pile response is quite different from that revealed in the lakebed zone of Mexico City. In the extremely soft clay deposit of the lakebed zone, almost the entire bending moment at the pile head was produced by ground motions (Iida 2013).

Thus, no contradictory building responses were obtained by the new building-response method in this and the preceding sections. On the other hand, some unreasonable building responses were provided by the two other methods. No contradictory building responses were obtained by the new method as well in the lakebed zone of Mexico

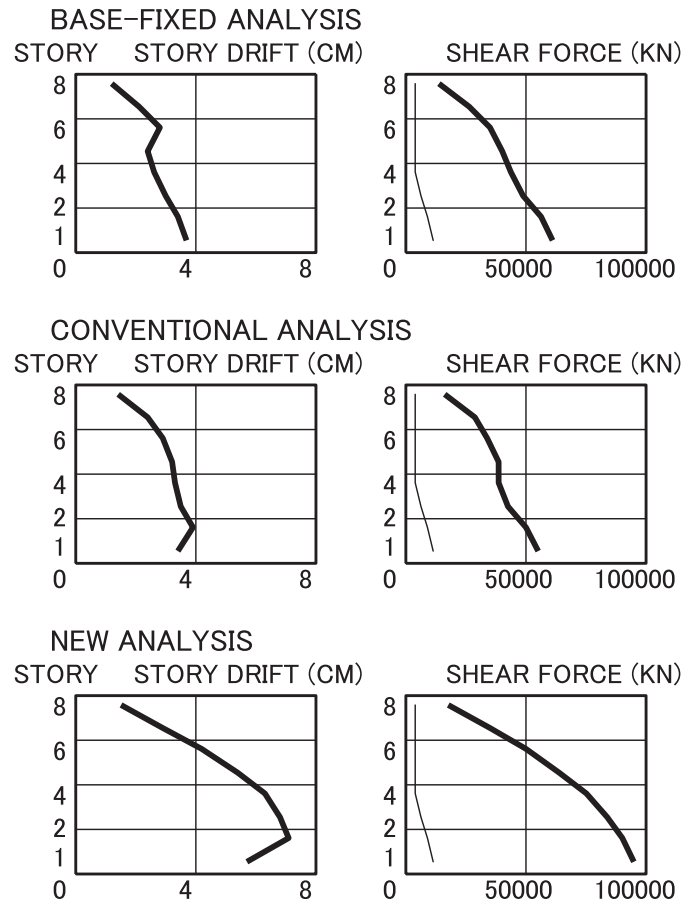


**Fig. 11.** Vertical distributions of maximum interstory drift and maximum shear force of the 8-story RC model building calculated by the three types of analyses at the Echujima station for the 1923 Kanto earthquake (thick lines; straight thin lines indicate yield strength)

City (Iida 2013). Accordingly, it is concluded that the new building-response method works satisfactorily in the linear range.

## Discussion

The serious limitations of input excitation as the inertial force for the soil-building interaction system were already clarified using model buildings in the lakebed zone of Mexico City in a recent study by Iida (2013). The degree of error in estimating building responses due to the input excitation in the lakebed zone with abnormally soft soils was much larger than that in the reclaimed zone of Tokyo Bay. Roughly speaking, the degree of error depends on the softness of soils and the amount of surface waves.

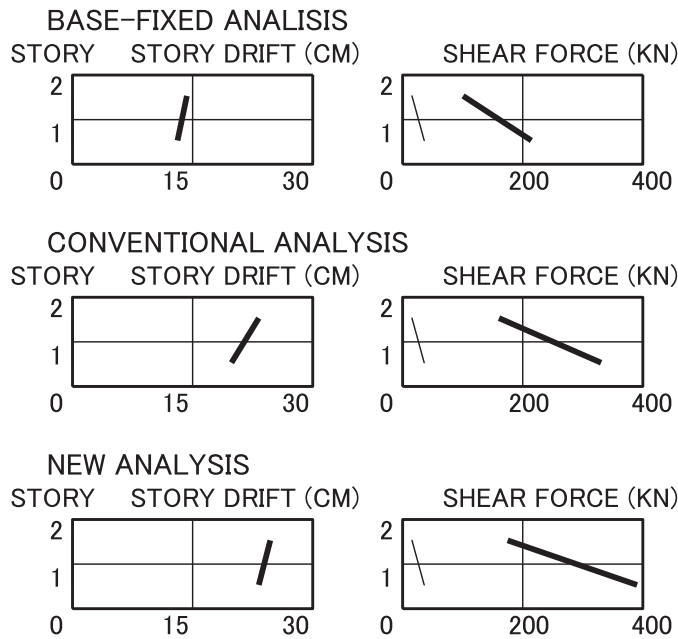


**Fig. 12.** Vertical distributions of maximum interstory drift and maximum shear force of the 2-story wood model building calculated by the three types of analyses at the Echujima station for the 1923 Kanto earthquake (thick lines; straight thin lines indicate yield strength)

**Table 6.** Maximum Response Values at Head of a Corner Pile of the 8-Story RC Model Building Calculated by the Two Types of Interaction Analyses at the Echujima Station for the 1923 Kanto Earthquake

Analysis	Shear force (kN)	Axial force (kN)	Bending moment (kN · m)
Conventional	4,146	26,676	5,850
New	7,634	31,850	10,290
New (removed) <sup>a</sup>	2,136	594	2,391

<sup>a</sup>In addition, pile response was calculated by the new analysis on the condition that only the superstructure was removed from the interaction system.

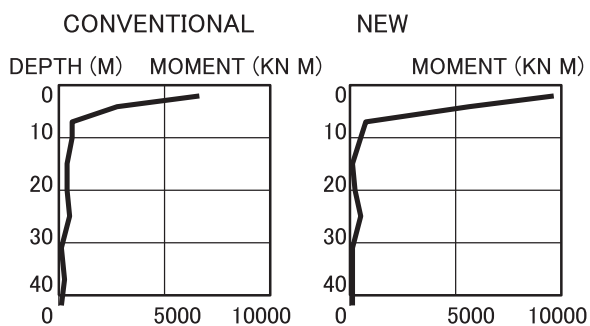


**Fig. 13.** Vertical distributions of maximum bending moment of a corner pile of the 8-story RC model building calculated by the two types of interaction analyses at the Echujima station for the 1923 Kanto earthquake

In this study, both the soil and building responses were treated in a linear fashion. The maximum soil strain reached  $5.2 \times 10^{-3}$  at the Echujima station for the Kanto earthquake, and it is considered that, in reality, the soil responses were not linear. Hence, the surface ground motions presumably were overestimated. Therefore, a nonlinear

response analysis of soils that can change a seismic wave field is required. Recently, nonlinear and liquefaction analyses for seismic soil-pile-structure interaction have become popular (e.g., Ashour and Norris 2003; Kim and Roesset 2004; Maheshwari and Sarkar 2011). In addition, it is considered that the linear building behavior in the analysis resulted in considerable overestimation of the maximum building responses (Tables 5 and 6). A nonlinear response analysis of buildings based on an input seismic wave field is required.

## Conclusions

A 3D linear soil-building interaction analysis based on an input seismic wave field was applied to estimate seismic building responses in the reclaimed zone of Tokyo Bay. The main conclusions of two simulations are as follows: (1) the first simulation successfully reproduced surface, downhole, and building accelerograms that were recorded at one borehole station during two medium-sized earthquakes; (2) in the second simulation, seismic responses of a midrise RC model building and a wood model building were favorably calculated at the other borehole station for the 1923 Kanto earthquake; and (3) the building responses also were compared with those calculated by a base-fixed building response analysis and by a conventional soil-building interaction analysis and demonstrated the superiority of the proposed method.

## Acknowledgments

Most of the accelerograms were provided as a data set of *Strong Motion Array Observation No. 2* by the Association for Earthquake Disaster Prevention of Japan. Parts of the accelerograms recorded at the Echujima station were supplied by Shimizu Corporation, Tokyo, Japan. The structural information on the real building and the building accelerograms recorded at the Toyo station were supplied by Takenaka Corporation, Tokyo, Japan. Dr. Tetsuya Ishihara of the Technical Research and Development Institute, JDC Corporation, Tokyo, Japan, gave helpful advice on the soil-building interaction system. Dr. Masaomi Teshigawara of Nagoya University gave instructive advice on buildings. The editor and four anonymous reviewers greatly improved the manuscript.

## Notation

The following symbols are used in this paper:

- $[C]$  = damping matrix;
- $D_s$  = base shear coefficient;
- $[H_K]$  = matrix of damping coefficients associated with stiffness;
- $[H_M]$  = matrix of damping coefficients associated with mass;
- $h_{BF}$  = damping coefficient used in the base-fixed response method;
- $h_{Kij}$  =  $ij$ th element of  $[H_K]$ ;
- $h_{Mij}$  =  $ij$ th element of  $[H_M]$ ;
- $h_{MO}$  = damping coefficient used in the conventional method for soil-building interaction;
- $h_{WFij}$  = damping coefficient used in the new method for soil-building interaction;
- $h_1$  = damping coefficient evaluated at the primary predominant period of the ground;
- $h_2$  = damping coefficient evaluated at the secondary predominant period of the ground;

- $[K]$  = stiffness matrix;  
 $[M]$  = mass matrix;  
 $M_j$  = earthquake magnitude; and  
 $\omega_1$  = primary angular frequency of the ground.

## References

- Abe, Y., et al. (1984). "Dynamic behavior of pile foundation during earthquakes." *Proc., 8th World Conf. on Earthquake Engineering*, Vol. III, International Association for Earthquake Engineering, Tokyo, 585–592.
- Architectural Institute of Japan. (1985). "Examination of analytical methods." *Proc., 1st Soil-Building Dynamic Interaction Symp.*, Tokyo, 77–81 (in Japanese).
- Ashour, M., and Norris, G. (2003). "Lateral loaded pile response in liquefiable soil." *J. Geotech. Geoenviron. Eng.*, 10.1061/(ASCE)1090-0241(2003)129:6(404), 404–414.
- Building Center of Japan. (2013). *The building standard law of Japan: Enforcement order*, Tokyo.
- Iida, M. (2006). "Three-dimensional linear and simplified nonlinear soil response methods based on an input wave field." *Int. J. Geomech.*, 10.1061/(ASCE)1532-3641(2006)6:5(342), 342–355.
- Iida, M. (2013). "Three-dimensional finite-element method for soil-building interaction based on an input wave field." *Int. J. Geomech.*, 10.1061/(ASCE)GM.1943-5622.0000232, 430–440.
- Iida, M., and Kawase, H. (2004). "A comprehensive interpretation of strong motions in the Mexican Volcanic Belt." *Bull. Seismol. Soc. Am.*, 94(2), 598–618.
- Iida, M., Yamanaka, H., and Yamada, N. (2005). "Wavefield estimated by borehole recordings in the reclaimed zone of Tokyo Bay." *Bull. Seismol. Soc. Am.*, 95(3), 1101–1119.
- Ishihara, T. (1994). "Seismic responses of two-dimensional nonlinear structure-pile-foundation-ground interaction systems based on three-dimensional systems." Ph.D. thesis, Yamaguchi Univ., Yamaguchi, Japan (in Japanese).
- Ishihara, T., and Miura, F. (1993). "Nonlinear seismic response analysis method for 3-D soil-structure interaction systems." *Proc. J. Soc. Civil Eng.*, 465(23), 145–154 (in Japanese).
- Kim, Y.-S., and Roesset, J. M. (2004). "Effect of nonlinear soil behavior on inelastic seismic response of a structure." *Int. J. Geomech.*, 10.1061/(ASCE)1532-3641(2004)4:2(104), 104–114.
- Kobayashi, K. (1989). "Seismic observation of a 10-story SRC building." *Proc., 2nd Soil-Building Dynamic Interaction Symp.*, Architectural Institute of Japan, Tokyo, 25–32 (in Japanese).
- Maheshwari, B. K., and Sarkar, R. (2011). "Seismic behavior of soil-pile-structure interaction in liquefiable soils: Parametric study." *Int. J. Geomech.*, 10.1061/(ASCE)GM.1943-5622.0000087, 335–347.
- Ohta, T., Niwa, M., and Ueno, K. (1978). "Seismic response characteristics of structure with pile foundation on soft subsoil layer." *Proc., 5th Japan Earthquake Engineering Symp.*, Architectural Institute Japan, Tokyo, 561–568 (in Japanese).
- Reza Tabatabaiefar, S. H., Fatahi, B., and Samali, B. (2013). "Seismic behavior of building frames considering dynamic soil-structure interaction." *Int. J. Geomech.*, 10.1061/(ASCE)GM.1943-5622.0000231, 409–420.
- Toki, K., and Fu, C. S. (1987). "Generalized method for non-linear seismic response analysis of a three dimensional soil–interaction system." *Earthquake Eng. Struct. Dyn.*, 15(8), 945–961.